International Journal of Fatigue 62 (2014) 119–132

Contents lists available at SciVerse ScienceDirect

International Journal of Fatigue

journal homepage: www.elsevier.com/locate/ijfatigue

A three-dimensional analysis of fatigue crack paths in thin metallic sheets

J.B. Esnault [a,b], V. Doquet [a,*], P. Massin [b]

[a] Laboratoire de Mécanique des Solides, CNRS, Ecole Polytechnique, Palaiseau, France
[b] LaMSid, UMR EDF – CNRS – CEA, Clamart, 1 Avenue du General de Gaulle, France

ARTICLE INFO

Article history:
Received 11 October 2012
Received in revised form 14 January 2013
Accepted 17 March 2013
Available online 4 April 2013

Keywords:
Fatigue crack
Shear lips
Thin sheet
Mixed-mode
X-FEM

ABSTRACT

Fatigue crack growth in thin sheets of 7075 T651 aluminium alloy and S355 steel were characterised in 3D, using crack front markings and topographic reconstructions of fracture surfaces. Tests performed in air or in salt water produced different crack paths for similar mechanical conditions, shear lips being reduced by corrosive environment, in the aluminium alloy as well as in the steel. Before the onset of shear lips development, tunnelling crack fronts were observed, due to the difference in closure effects at mid-thickness and near free surfaces. Tunnelling was progressively reduced and cancelled as slanted crack growth developed, even though ΔK_I was reduced locally by crack twisting. This indicates a significant contribution of shear modes to the crack driving force, even though mode I striations are present in slanted zones. Elastic three-dimensional X-FEM computations were performed to analyse the observed crack growth kinetics, based on ΔK_I, ΔK_{II} and ΔK_{III}. The crack growth rates correlated much better to $\Delta K_{eq} = \sqrt{\Delta K_I^2 + \Delta K_{II}^2 + \frac{\Delta K_{III}^2}{(1-\nu)}}$ than to ΔK_I. Elastic–plastic finite element simulations and the local application of a fatigue criterion with an amplitude-dependent critical plane were found to capture qualitatively the transition in fracture mode and its inhibition by side grooves.

1. Introduction

Fatigue crack growth normal to the tensile axis becomes unstable in thin metallic sheets, above a material and environment-dependent loading amplitude, even though, in many cases, small scale yielding conditions still prevail. Tilting and twisting of the crack path starts from side surfaces (Fig. 1). Under a constant or increasing loading range, the deviated parts of the crack, called "shear lips" progressively grow inward, so that the crack finally becomes fully slanted.

Shear lips development has been investigated mainly in aluminium alloys by Schijve and co-workers [1–3] or Zuidema et al. [4–6], while very few studies were devoted to steel [7] or titanium alloys [8]. These authors observed that shear lips started to develop above a threshold crack growth rate. This threshold rate would be 5–7.5 μm/cycle in titanium alloys, according to Walker et al. [8] and 0.2–0.7 μm/cycle for 7075-T6 aluminium alloy, according to Hudson and Scardina [9].

Shanyavsky and Koronov [10] measured the shear lips width in thin aluminium alloy cruciform specimens cyclically loaded in two orthogonal directions and reported that a positive biaxiality ratio reduced the shear lips, while a negative ratio increased it. They also observed a reduction in shear lips width when the R ratio increased. This observation conflicts with the conclusion of Zuidema et al. [4–6] that the "steady-state" shear lips is a linearly increasing function of the effective ΔK, which usually increases with R.

Van Kranenburg [11] reports that side grooves inhibit crack deviation in aluminium alloys. Note that the suppression of shear lips is associated with modifications of the crack front shape: shallow side grooves produce straight crack fronts instead of tunnelling fronts in smooth specimens in which shear lips develop. Deep and sharp side grooves even produce concave fronts (Figs. 4–6 in [11]). The relationship between crack front curvature and the onset of crack deviation will be discussed below.

Walker et al. [8] first reported an influence of environment on shear lips development in titanium alloys. A 3.5% NaCl solution appeared to postpone crack twisting in Ti–8Al–1Mo–1V, while no systematic effect was found in Ti–6Al–4V. Vogelesang and Schijve [2] observed complete crack twisting for a lower ΔK_I in vacuum than in air and for a higher ΔK_I in salt water for 7075 T651 aluminium alloy. Horibe et al. [7] reported a similar effect of salt water in low strength steel, but a less pronounced effect of environment in high strength steel.

With all the above-mentioned work, the development of shear lips in fatigue might seem well documented. However, most anal-

* Corresponding author. Tel.: +33 1 69 33 57 65; fax: +33 1 69 33 57 06.
E-mail address: doquet@lms.polytechnique.fr (V. Doquet).

0142-1123/$ - see front matter © 2013 Elsevier Ltd. All rights reserved.
http://dx.doi.org/10.1016/j.ijfatigue.2013.03.015

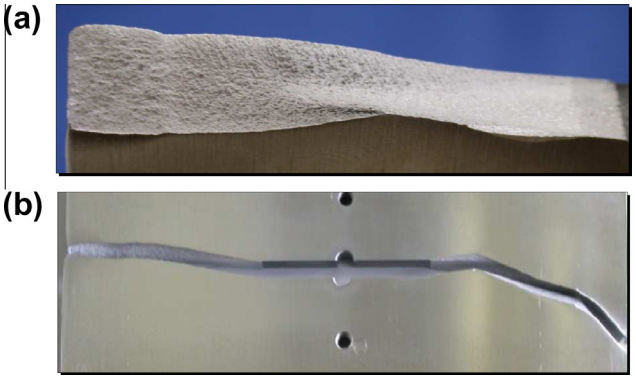

Fig. 1. Typical aspect of a slanted crack: (a) twisted fracture surface and (b) tilted crack on the side surface.

yses of experimental data available in the literature are two-dimensional. Slanted crack growth kinetic data was analysed as if it was mode I and as if the growth rate and driving force were uniform along the front. Based on "constant ΔK_I tests", empirical relations between the steady-state shear lips width, the loading frequency and the "effective ΔK_I" were derived for aluminium alloys [4,5]. This parameter will be denoted below by "apparent effective ΔK_I", since it was computed in 2D for a normal crack of the same length as that observed on the free surface, with a correction for closure effects. This correction was a polynomial function of the R ratio valid for mode I, while crack deviation is expected to modify substantially the closure effects. The meaning of "constant ΔK_I tests" is also questionable in view of the large gradient in K_I, K_{II} and K_{III} along the front of a partially or completely slanted crack (see below) and of the important drop in ΔK_I associated with crack twisting.

In an effort toward 3D analysis, Pook [12,13] performed finite element computations of the stress intensity factors along the front of a fully slanted crack in specimens of different thickness and found a symmetric profile of K_I and K_{III} (the former being highest at mid-thickness, and the latter near the surface, where both were nearly equal) plus a skew-symmetric profile of K_{II}. K_I for the slanted crack was 0.51–0.71 smaller than its apparent value (computed in 2D for a normal crack of same length). He suggested that the onset of shear lips development from the free surfaces was controlled by the extent of the area dominated by the corner-point singularity compared to some microstructural dimension. Bakker [14] also performed some 3D finite element computations of stress intensity factors for fully or partially slanted crack. However, as in the problem studied by Pook, a straight crack front was considered, which is not realistic in fatigue. Materna and Oliva [15] recently performed 3D elastic–plastic simulations with periodic node release to analyse the stress and strain state ahead of a partially slanted propagating crack, with a steady-state shape and growth direction. They considered a tunnelling front in the central normal part and a straight front in the slanted parts of fixed width. They found much larger crack tip plastic zones in slanted areas – where modes II and III were important – than in the normal part. They concluded that: "Common criteria for prediction of the mixed-mode crack propagation direction fail for the shear lips area".

The present work re-examines the problem from a 3D perspective, in order to determine what mechanical parameters control the onset of crack deviation and the kinetics of slanted crack growth. Since environment seemed to influence shear lips development, a 3D experimental characterisation of the crack paths and kinetics was performed, both in air and in salt water, associated to a comparison of the respective 3D crack paths.

A 3D numerical analysis of the crack growth rates was done, based on linear elastic fracture mechanics, taking into account mode-mixity. Elastic–plastic computations of stress and strain fields ahead of the crack front were used to rationalise the observed crack paths. A method to predict the onset of crack twisting and the twist angles was also proposed.

2. Experimental procedures

Fatigue crack growth tests were performed with a frequency of 5 Hz and an R ratio equal to 0.1 on 6 mm-thick, 100 mm-wide, 300 mm-high Centre Crack Panel specimens. Two material were investigated: 7075-T651 aluminium alloy ($\sigma_{y(0,2)} = 376$ MPa, $\sigma_u = 537$ MPa, $E = 75$ GPa) and S355 low-alloy steel ($\sigma_{y(0,2)} = 349$ MPa, $\sigma_u = 510$ MPa, $E = 205$ GPa) with the chemical composition indicated in Table 1. In both cases, the tensile axis was parallel to the rolling direction.

Both sides of the specimens were polished to allow crack propagation monitoring with an optical microscope, at a magnification of one hundred. Tests were performed either in air or in a transparent reservoir filled with a 3.5 g/l NaCl solution, under constant loading amplitudes indicated in Table 2. The maximum applied stress represented 10–12% of the yield stress for the aluminium alloy. With such a loading range, based on 3D F.E. computations for a normal crack, the requirement that both the crack length and the length of the uncracked ligament should be larger than 25 times the plastic zone size, for small-scale yielding were satisfied along the whole crack front. For steel, the maximum applied stress represented 32% of the yield stress. With this loading range, the criterion was satisfied up to a crack length of 28 mm (between the 7th and 8th marker block).

Ten to twelve marker block loading sequences, with K_{max} unchanged but $K_{min} = 0.7K_{max}$ were applied at specified cycle numbers, denoted by Nm_i ($i = 1$–12), until approximately 100 μm propagation was achieved. This marked the position of the crack front on the fracture surface (see Fig. 5 below) and allowed us to derive the average crack lengths $a(Nm_i)$ and the mean crack growth rate between consecutive markings, for any point along the front, as explained below. Fourth to sixth degree polynomial equations were adjusted to describe the shape of each front in the numerical simulations. To characterise crack front tunnelling, the difference Δa in crack length between the mid-thickness and the average length on the free surfaces was measured.

The three-dimensional topography of the fracture surfaces was reconstructed, thanks to digital optical microscopy (Fig. 2). A fifty-fold magnification was used for image capture and 13 images had to be stitched to map the whole crack path from the notch root to the onset of ductile fracture. The results were obtained as (x,y,z) triplets, where x denotes the distance from the notch root along the free surface, y, the position in depth, and z the height from the notch plane, with a spatial discretization of 4.5 μm * 4.5 μm in the x–y plane and 35 μm in the z direction. Longitudinal and transverse height profiles, $z(x)$ or $z(y)$ were derived. Polynomial expressions were fitted to these profiles and used to compute the local *tilt* and *twist* angles as $\phi = \arctan(dz/dx)$ and $\theta = \arctan(dz/dy)$, respectively. The shear lips width, denoted by t_s, was deduced as the width of the zone where $|\theta| \geqslant 4°$. Such a quantitative criterion was introduced because a direct determination of the width of normal and slanted parts of the crack from the transverse

Table 1
Chemical composition of the materials (wt%).

7075-T6	Si	Fe	Mn	Mg	Zn	Cr
	0.08	0.2	0.01	2.8	6.1	0.25
S355	C	Mn	Si	P	S	N
	0.17	1.7	0.6	0.055	0.055	0.11